

## Hartree-Fock microscopic description of band structures in $^{99}\text{Pd}$

Z. Naik<sup>2</sup>, S. Sihotra<sup>1\*</sup> and J. Goswamy<sup>1</sup>

<sup>1</sup> Department of Physics, Panjab University, Chandigarh-160 014, India

<sup>2</sup> Department of Physics, Sambalpur University, Sambalpur-768 019, India

\* email: ssihotra@gmail.com

### Introduction:

The nuclei approaching the neutron and proton major shell closures at  $N=Z=50$  provide unique opportunity to study interplay between the single-particle and collective degrees of freedom, and influence of the valence orbitals on deformation. Various new deformation generating mechanisms have been identified in theoretical interpretation of the observed band structures [1]. Investigations reveal diversity in band structures with configurations resulting from the coupling of the  $g_{9/2}$ ,  $d_{5/2}$ ,  $g_{7/2}$ , and  $h_{11/2}$  valence nucleons and the core-excited (particle-hole) pairs. For the nuclei approaching  $Z = 50$  from below, the proton Fermi surface lies near the high- $\Omega$  orbitals of the intruder  $\pi g_{9/2}$  subshell, which drive the nuclear shape towards oblate deformation. Strongly prolate-driving low- $\Omega$   $\nu h_{11/2}$  subshell orbitals are accessible at low excitation energies for the nuclei receding above the  $N = 50$  shell closure. Rotational bands built on the core-excited configurations terminating at low energy are also observed. The observed collective states have been interpreted as proton particle-hole excitations across the major shell gap made energetically possible by the combination of strong proton-pair correlations and possibly proton-neutron interaction, which is most effective for spin-orbit partner orbitals, viz.,  $\pi g_{9/2}$  and  $\nu g_{7/2}$ . Furthermore, the delicate interplay of strongly shape driving  $\pi g_{9/2}$  and  $\nu h_{11/2}$  orbitals can influence the overall shape of the nucleus, and result in  $\gamma$ -soft (triaxial) shapes with modest deformation  $\beta_2 \approx 0.15$ . The relevant intriguing triaxiality based phenomena such as magnetic rotation and degenerate twin bands have been reported in this mass region. The twin degenerate dipole bands with similar energy staggering and electromagnetic strengths were explained with aplanar tilted rotation of the triaxial core along with the valence neutrons and protons aligned along the two extreme axes of

the core. Specific noncollective aligned states with the nuclear spin made up completely from angular momentum contributions of the particles and holes in open shells are able to compete energetically with weakly deformed collective structures. The maximally aligned states have been observed in the  $^{98,99}\text{Ag}$  [2, 3] and  $^{98,102,103}\text{Pd}$  [4] isotopes. In  $^{102}\text{Pd}$ , four band structures have been observed up to termination and interpreted in terms of valence-space and core-excited configurations. Several terminating configurations have also been identified in various isotopes of  $^{44}\text{Ru}$  and  $^{45}\text{Rh}$ , and  $^{52}\text{Te}$  and  $^{53}\text{I}$ , and recently in  $^{123}\text{Cs}$ .

Excited states in  $^{99}\text{Pd}$  nucleus were populated in fusion-evaporation reaction  $^{75}\text{As} (^{28}\text{Si}, p3n)$  at  $E_{\text{lab}}=120$  MeV. The de-excitations have been investigated through in-beam  $\gamma$ -ray spectroscopic techniques. The  $^{28}\text{Si}$  beam was delivered by the 15UD Pelletron accelerator at Inter University Accelerator Centre (IUAC), New Delhi. The deexciting  $\gamma$ -rays were detected using the Indian National Gamma Array (INGA) at IUAC equipped with 18 clover detectors [5]. In the offline analysis, the level scheme of  $^{99}\text{Pd}$  was established using the energy, intensity and coincidence relationships for various gamma transitions, and the angular correlation and polarization analyses.

### Results and discussion

Low excitation bands in an odd-A nucleus in the near spherical  $A \sim 100$  mass region are relatively easier to identify because of the limited number of possible shell-model configurations. In case of  $^{99}\text{Pd}$  ( $Z = 46$ ,  $N = 53$ ), there are 4 proton holes in the  $g_{9/2}$  orbital and 3 neutrons outside the  $N = 50$  shell closure. The level scheme is established up to excitation energy  $\sim 11.5$  MeV and spin  $\sim 25\hbar$  with the addition of about sixty new transitions. We have obtained three new bands at high spins (labeled as B2', B3, B4).

The observed level structures in the  $^{99}\text{Pd}$  nucleus have been studied using the Projected Hartree-Fock (PHF) technique. In the deformed Hartree-Fock and angular-momentum projection (PHF) calculations, the HF equation is derived from nuclear Hamiltonian consisting of the single-particle terms and the two-body interaction terms, and solved to get the single particle orbits of nucleons. The model space considered here is outside the inert spherical core with  $Z = 40$  and  $N = 40$ . The surface delta (SD) interaction with strength  $V_{pp} = V_{np} = V_{nn} = 0.34$  MeV is taken as the two-body residual interaction among six active protons and thirteen active neutrons. The spherical single particle orbits considered in the PHF calculations are  $3s_{1/2}$ ,  $2d_{3/2}$ ,  $2d_{5/2}$ ,  $1g_{7/2}$ ,  $1f_{7/2}$ ,  $1g_{9/2}$ , and  $1h_{11/2}$  with energies 2.129, 3.109, 0, 1.82, 7.596, -4.0484, and 3.066 MeV, respectively, for protons and  $3s_{1/2}$ ,  $2d_{3/2}$ ,  $2d_{5/2}$ ,  $2f_{7/2}$ ,  $1h_{9/2}$ , and  $1h_{11/2}$  with energies 2.008, 2.715, 0, 1.515, 7.763, -3.996, and 2.96 MeV, respectively, for neutrons. The level scheme at lower angular momentum consists of B1 and B2 bands, which are based on singles particle  $\nu g_{9/2}$  and  $\nu d_{5/2}$  orbitals. The previously observed  $11/2^-$  state at 2017 keV is identified to be  $\nu h_{11/2}$ . The  $9/2^+$  level at 1102 keV is based on the  $\nu g_{9/2}$  hole. An interesting result of the present work is fully aligned states at  $39/2^-$  and  $31/2^+$  states of band B3 and band B4, respectively with  $[\pi(g_{9/2})^{-2} \otimes \nu(g_{7/2})^2 \otimes \nu(h_{11/2})]$  and  $\pi(g_{9/2})^{-2} \otimes \nu g_{7/2} \otimes \nu(d_{5/2})^{-2}$  or  $[\pi(g_{9/2})^{-2} \otimes \nu(g_{7/2})^3]$  configurations, respectively.

The excited positive-parity band B4 has been reproduced by for two configurations (a)  $\nu(g_{7/2})^2 \otimes \nu(h_{11/2})^2 \otimes \nu(g_{9/2})^{-1} \otimes (\pi g_{9/2})^6$  with  $K = 5/2^+$  state, and (b) one obtained by exciting one  $g_{9/2}$  proton to  $\Omega = 1/2^+$   $g_{7/2}$  orbit, i.e.,  $\nu(g_{7/2})^2 \otimes \nu(h_{11/2})^2 \otimes (\nu g_{9/2})^{-1} \otimes \pi(g_{9/2})^5$ ;  $\otimes \pi(g_{7/2})$  configuration with  $K = 19/2^+$ . The lowest observed state in band B4 is  $19/2^+$ , which favors the (b) configuration. The excited negative-parity band B3 are closely followed for two configurations (a) one obtained by mixing the  $(\pi g_{9/2})^6 \otimes \nu(g_{9/2})^{10} \otimes \nu(g_{7/2})^2 \otimes \nu h_{11/2}$  configuration with  $K=1/2^-$  and  $K=3/2^-$ , and (b) the second obtained by mixing the  $K=1/2^-$  configuration obtained by coupling of  $(\pi g_{9/2})^6 \otimes \nu(g_{9/2})^8 \otimes \nu(g_{7/2})^2 \otimes \nu h_{11/2}$  configurations with  $K=1/2^-$  and  $K=3/2^-$ , and (b) the second obtained by mixing the  $K=1/2^-$  configuration

obtained by coupling of  $(\pi g_{9/2})^6 \otimes \nu(g_{9/2})^8 \otimes \nu(g_{7/2})^2 \otimes \nu(d_{5/2})^2 \otimes (2p-2h)$  to  $\nu h_{11/2}$  to its excited configuration with  $K=3/2^-$ . These plots are shown in Fig. 1.

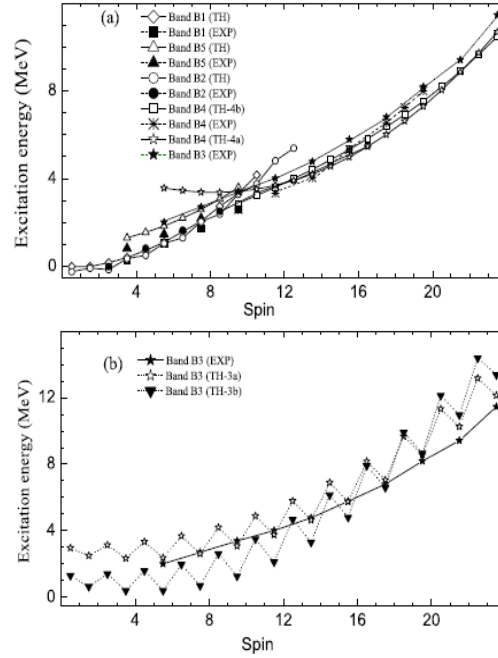


**Fig. 1** Comparison of the observed energy levels of (a) bands B1, B2, B4, and B5, and (b) band B3, of  $^{99}\text{Pd}$  with the PHF calculations.

## References

- [1]. S. Lalkovski *et al.*, Phys. Rev. C **71**, 034318 (2005).
- [2]. W. Reviol *et al.*, Nucl. Phys. **A557**, 391C (1993).
- [3]. J. Gizon *et al.*, Z. Phys. A **345**, 335 (1993).
- [4]. J. Cederkall *et al.*, Z. Phys. A **359**, 227 (1997).
- [5]. S. Muralithar *et al.*, Nucl. Instrum. and Methods A **622**, 281(2010).